Prioritized neural processing of social threats during perceptual decision-making

M. El Zein, Rocco Mennella, M. Sequestro, E. Meaux, V. Wyart, J. Grèzes

Article

Prioritized neural processing of social threats during perceptual decision-making

M. El Zein, R. Mennella, M. Sequestro, E. Meaux, V. Wyart, J. Grèzes

marwaelzein@gmail.com (M.E.Z.)
julie.grezes@ens.psl.eu (J.G.)

Highlights

Emotion vs. color detection tasks on the same two-dimensional visual stimuli

Earlier EEG encoding of threat dimension during the emotion task

Earlier prediction of choices in mu-alpha rhythm during the emotion task

Support for the motivational value of socially relevant signals

Article

Prioritized neural processing of social threats during perceptual decision-making

M. El Zein,[1,2,3,4,]* R. Mennella,[1,5] M. Sequestro,[1] E. Meaux,[1] V. Wyart,[1,6,7] and J. Grèzes[1,7,8,]*

SUMMARY

Emotional signals, notably those signaling threat, benefit from prioritized processing in the human brain. Yet, it remains unclear whether perceptual decisions about the emotional, threat-related aspects of stimuli involve specific or similar neural computations compared to decisions about their non-threatening/non-emotional components. We developed a novel behavioral paradigm in which participants performed two different detection tasks (emotion vs. color) on the same, two-dimensional visual stimuli. First, electroencephalographic (EEG) activity in a cluster of central electrodes reflected the amount of perceptual evidence around 100 ms following stimulus onset, when the decision concerned emotion, not color. Second, participants' choice could be predicted earlier for emotion (240 ms) than for color (380 ms) by the mu (10 Hz) rhythm, which reflects motor preparation. Taken together, these findings indicate that perceptual decisions about threat-signaling dimensions of facial displays are associated with prioritized neural coding in action-related brain regions, supporting the motivational value of socially relevant signals.

INTRODUCTION

Accurate decoding of socially relevant information emitted by others, such as emotional expressions, is crucial to guide adaptive decisions. Indeed, social signals are granted preferential processing: people quickly allocate attention to human faces and bodies in natural scenes,[1] detect changes in faces better than in non-social objects,[2] and respond faster to social than to non-social hazards.[3] Emotional expressions, especially when they signal threat, are further prioritized relative to neutral displays and to non-social stimuli.[4–6] Social threat signals, such as angry or fearful facial expressions, are associated with perceptual and attentional advantages[6–11] and they also modify the perception of surrounding environment.[12–15] Moreover, they shape the observer's behavior, by increasing motor preparation[16–22] and by influencing approach/avoidance decisions.[23–27]

Perceptual decisions made on non-socioemotional characteristics of stimuli show that stimulus evidence is encoded over associative, centroparietal regions (CPP, gradual buildup starting from 170 ms after stimulus onset) and over motor regions (lateralized readiness potential - LRP, gradual buildup from 320 ms, both CCP and LRP peak around 400-500 ms,[28,29] see also[30–36]). Interestingly, recent experiments investigating perceptual decisions on morphed emotional displays also revealed that the brain areas specialized in the processing of human faces feed information forward to the dorsal stream where sensory evidence accumulates and to the premotor regions where decisions emerge.[37–40] Moreover, when directly comparing perceptual decision on high- and low-threat facial displays, El Zein et al.[41] found that high-threat displays elicited earlier (∼200 ms) and enhanced stimulus neural encoding in both associative and motor regions simultaneously. Despite the similarity in the neural dynamics underlying perceptual decisions on threatening and neutral stimuli, the question remains whether stimulus encoding is faster over centroparietal and motor areas during perceptual decisions on socioemotional versus non-emotional stimuli.

Several methodological constraints in previous research have precluded a direct comparison between these two types of stimuli. Past studies have focused either on perceptual decisions on emotional displays[37,38,41–44] or on social vs. non-social stimuli.[45–51] To our knowledge, only one study has compared decisions on static facial displays of emotion and animal pictures and concluded that there is a common neural signature for emotional and non-emotional decisions under perceptual ambiguity.[52] However, by focusing only on the late positive potential (LPP, beginning ∼400 ms after stimulus onset), this study does not provide information about early processing steps, making it impossible to determine whether the processing of emotional stimuli is prioritized over non-emotional ones. Furthermore, neither the amount of perceptual evidence nor the detection sensitivity across stimuli was equalized between the two tasks. Therefore, no previous study has precisely
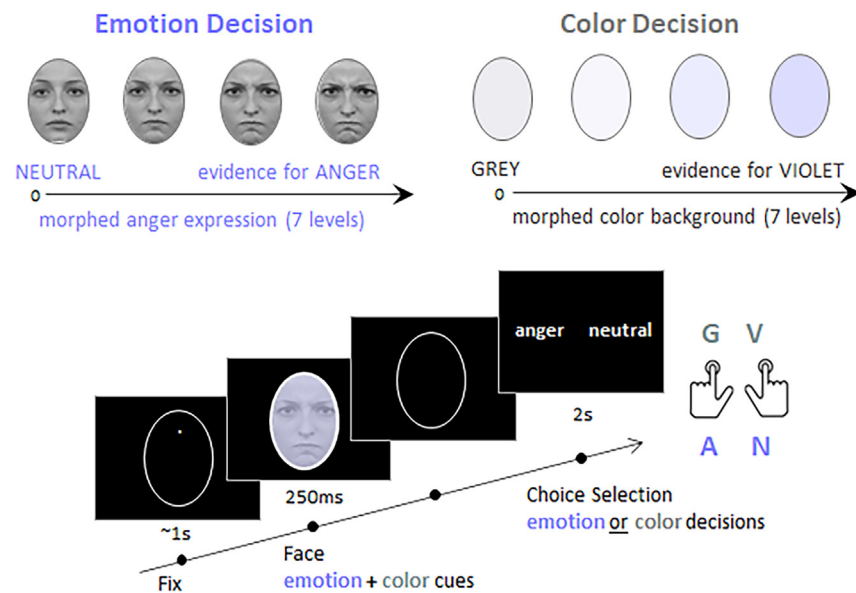
Figure 1. Stimuli and experimental procedure

The top panel shows examples of morphed anger expressions and color masks used to orthogonally manipulate the strength of perceptual evidence in the stimuli. Note that only four of the seven levels of morphs created from neutral to anger and from grey to violet are presented. The bottom panel illustrates the time course of one trial during perceptual detection tasks. After a fixation period, a morphed face, on top of which is superimposed a morphed color mask, was displayed for 250 ms. After face offset, and depending on the block, participants reported the presence or absence of either emotion (anger) or color (violet) in the stimuli, while ignoring the other task-irrelevant dimension.

characterized, within participants, the neural mechanisms involved in making decisions about perceptual stimuli that simultaneously vary on threat and another non-threatening neutral dimension in a controlled, equalized way.

To reach a comprehensive understanding of whether threat expressions are prioritized during decision-making, we have developed a novel electroencephalography (EEG) paradigm in which participants performed two different detection tasks (emotion vs. color) on the same, two-dimensional visual stimuli. We orthogonally manipulated the strength of perceptual evidence in the stimuli by presenting morphed facial expressions (from neutral to angry) with a morphed color background (from grey to violet). In different blocks, participants were asked to report the presence or absence of either emotion (anger) or color (violet) in the stimulus, while ignoring the other task-irrelevant dimension (see Figure 1). We used facial expressions of anger as threat stimuli signaling potentially harmful intentions. Since the association of angry faces with direct and averted gaze has been shown to be appraised as high and low threat, respectively[53–56] we manipulated the contextual significance of the displayed emotion via changes in gaze direction. Gaze direction was never mentioned to participants and was irrelevant to task performance. Importantly, to closely match emotion and color perceptual detection tasks, we not only equalized the amount of sensory evidence in the stimuli across tasks using morph matching, but also equalized participants detection sensitivity across the two stimulus dimensions (emotion and color) using an adaptive Bayesian titration procedure.

We hypothesized (Hypothesis 1 - H1) earlier selective neural encoding of the threat-related dimension (defined here as co-variation between neural activity and perceptual features of the stimulus) in the emotion task, as compared to the encoding of the color dimension in the color task; and (H2) earlier prediction of choice in motor-related signals in the emotion task compared to the color task. Finally, we expected that both information processing (H3a) and choice prediction (H3b) should be stronger for high compared to low threat signals, i.e., for angry faces associated with direct gaze compared to averted gaze.[17,41,57,58]

RESULTS

Behavioral results from the emotion vs. color task

For emotion and color decisions separately, we fitted participants' behavior with a noisy, 'signal detection'-like psychometric model (inspired by the Signal Detection Theory - SDT) that could account for each observer's decisions, and extracted the sensitivity parameter, which reflects the observer's sensitivity to sensory information, and the response bias parameter, which reflects the observer's tendency to interpret the stimulus as displaying either one of the two options (anger or neutral for emotion decisions, violet or grey for color decisions). In order to test our first hypothesis, i.e., earlier neural encoding of stimulus strength in the emotion task than in the color task, we needed to ensure that any neural difference was not due to differences in detection sensitivity between the tasks. Therefore, we used a Bayesian titration procedure to ensure equal sensitivity across tasks (see STAR methods for details). As displayed in Figure 2A (left panel), the titration procedure was successful in equalizing the detection sensitivity between the two tasks, as the sensitivity parameter in the emotion task (0.63 ± 0.16) did not significantly
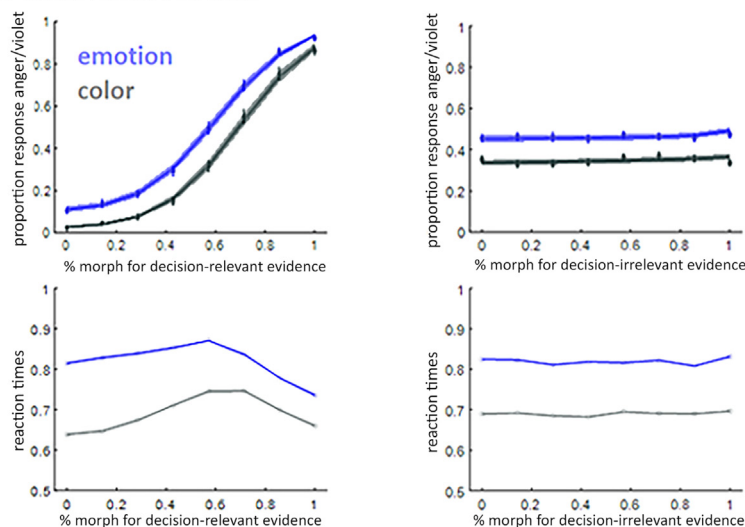
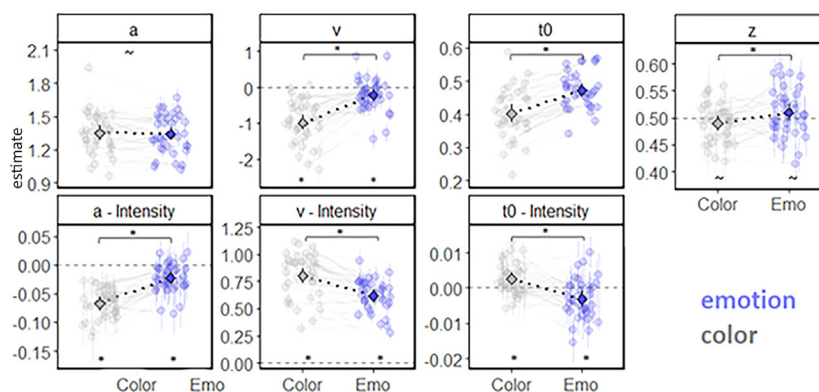**Figure 2. Behavioral results**

(A) The top-left panel shows the psychometric function representing the proportion of 'anger' (in blue) or 'violet' (in grey) responses as a function of the strength of the decision-relevant perceptual evidence for anger or violet (percentage of morph, 0 = neutral or grey, 100% anger or violet). Dots and attached error bars indicate the experimental data (mean ± sem). Lines and shaded error bars indicate the prediction of the fitting model. The bottom-left panel represents mean reaction times as a function of the strength of perceptual evidence for anger or violet. Top- and bottom-right panels present the psychometric function representing the proportion of 'anger' or 'violet' responses (top) and mean reaction times (bottom) as a function of the strength of the decision-irrelevant perceptual evidence (i.e., emotion intensity in color decisions, and color intensity in emotion decisions).

(B) Drift-diffusion model results. The best-fitting model included the effect of task, intensity level, and their interaction on threshold (a), drift rate (v), and non-decision time (t0), and an effect of task on starting point bias (z). Light points and lines: Individual estimates and 95% Credible Interval. Dark points and lines: Group level estimates and 95% Credible Interval.

differ from that in the color task (0.64 ± 0.17) (T_{37} = 0.33, p = 0.73, d = −0.073, BF = 0.187). However, there was a difference in the bias parameter between the emotion (−2.69 ± 0.64) and the color tasks (−3.16 ± 0.99) (T_{37} = 2.40, p = 0.02, d = 0.562, BF = 2.209), and we therefore accounted for the choice at each trial in our encoding regressions. Participants were also faster in the color task (mean ± sem: 690 ± 39 ms) as compared to the emotion task (mean ± sem: 820 ± 46 ms) (T_{36} = −9.264, p < 0.001, d = 1.119, BF = 2.1267e+08) (Figure 2A – left panel).

We then examined whether responses and reaction times changed as a function of the irrelevant dimension (color intensity in the emotion task, emotion intensity in the color task). There was no interference, as the percentage of anger choices did not vary with color intensity nor did the associated reaction times, and the percentage of violet choices did not vary with anger intensity, nor did the associated reaction times (Figure 2A – right panel).

Drift-diffusion model results

Because the SDT framework is static over time, we further investigated these behavioral differences by fitting and comparing different drift-diffusion models (DDMs[59]). DDMs assume that sensory evidence for competing choices accumulates over time until a decision boundary is

reached. By modeling choice and response times together, DDMs allowed inferring the cognitive processes involved in our two binary decision tasks by estimating a set of parameters that describe the dynamic decision process, including the rate of evidence accumulation (drift rate v), the distance between the two response boundaries (threshold a), the starting point of the decision between the two alternatives (starting point bias; z), as well as the time required for stimulus encoding and response execution (non-decision time t0).

The best-fitting model included the effect of task, intensity level, and their interaction on threshold (a), drift rate (v), and non-decision time (t0), and an effect of task on starting point bias (z) (see Figure 2B). The three chains converged properly (maximum R-hat = 1.009; minimum Effective Sample Size = 1026; the 'hairy caterpillar' shape was visually verified), and the simulated data showed a high correlation with the observed data (Anger/Violet response proportion: r_{col} = 0.998, r_{emo} = 0.998; Anger/Violet RTs: r_{col} = 0.955; r_{emo} = 0.977; Neutral/Grey RTs: r_{col} = 0.989; r_{emo} = 0.985) (see supplementary text for detailed information about model diagnostic).

Regarding the starting point bias (z), although the posterior parameters indicated a credibly small difference between the Color and Emotion tasks ($z_{col-emo}$ = −0.021; 95%CrI = [-0.041, −0.0001]; posterior probability $pp_{(z\ col-emo>0)}$ = 0.024), with a lower starting point in the Color task compared to the Emotion task, neither the starting point for the Color task (z_{col} = 0.489; 95%CrI = [0.475, 0.503]; $pp_{(z\ col\ >.5)}$ = 0.058) nor that for the Emotion task (z_{emo} = 0.510; 95%CrI = [0.494, 0.525]; $pp_{(z\ emo>.5)}$ = 0.896) was credibly different from 0.5. This pattern suggests that even if participants were slightly more likely to choose Angry rather than Neutral compared to Violet rather than Grey, they did not exhibit a credible response bias in either task.

With respect to the threshold parameter (a), the posterior parameters showed no credible difference between tasks ($a_{col-emo}$ = 0.008; 95%CrI = [−0.079, 0.098]; $pp_{(a\ col-emo>0)}$ = 0.574). However, the continuous effect of Intensity was credible in both the Color task (β_{col} = −0.068; 95%CrI = [−0.080, −0.056]; $pp_{(\beta col>0)}$ = 0) and the Emotion task (β_{emo} = −0.023; 95%CrI = [−0.034, −0.012]; $pp_{(\beta\ emo>0)}$ = 0), with greater intensity being associated with a lower threshold in both tasks. Furthermore, the effect of intensity was credibly more negative in the Color task compared to the Emotion task ($\beta_{col-emo}$ = −0.045; 95%CrI = [−0.061, −0.028]; $pp_{(\beta\ col-emo>0)}$ = 0), suggesting that the lowering of response threshold with increasing intensity level was present in both tasks, but with a smaller effect in the Emotion task.

Regarding the drift rate (v), the posterior parameters revealed that both the drift rate for the Color task (v_{col} = −0.987; 95%CrI = [−1.194, −0.778]; $pp_{(v\ col>0)}$ = 0) and for the Emotion task (v_{emo} = −0.211; 95%CrI = [−0.370, −0.048]; $pp_{(v\ emo>0)}$ = 0.006) were credibly lower than 0. Furthermore, the drift rate in the Color task was credibly lower than in the Emotion task ($v_{col-emo}$ = −0.778; 95%CrI = [-1.038, −0.510]; $pp_{(v\ col-emo>0)}$ = 0). Given that these estimates represent the parameter at the level 0 of intensity, these results suggest that for these ambiguous stimuli, participants favored the decision toward the Grey and Neutral boundaries, and that this effect was stronger during the Color task. We additionally found a credible effect of Intensity for both the Color (β_{col} = 0.804; 95%CrI = [0.731, 0.876]; $pp_{(\beta\ col>0)}$ = 1) and the Emotion task (β_{emo} = 0.619; 95%CrI = [0.565, 0.672]; $pp_{(\beta\ emo>0)}$ = 1), and a credible difference of these effects between the tasks ($\beta_{col-emo}$ = 0.186; 95%CrI = [0.094, 0.275]; $pp_{(\beta\ col-emo>0)}$ = 1), with a stronger effect of intensity in the Color task. Therefore, as expected, increasing morph intensity toward a Violet or Angry stimulus led participants to more efficient evidence sampling toward that boundary, and this effect was stronger during the Color task.

Finally, posterior parameters for the non-decision time (t0) showed a credible difference in the non-decision time between the tasks ($t0_{col-emo}$ = −0.070; 95%CrI = [−0.103, −0.037]; $pp_{(t0\ col-emo>0)}$ = 0), with more time required to encode the stimulus and/or execute the response in the Emotion task. Interestingly, we found the Intensity effect to be credible for both the Color and for the Emotion tasks. However, while non-decision time increased with intensity for the Color task the (β_{col} = 0.003; 95%CrI = [0.001, 0.004]; $pp_{(\beta\ col>0)}$ = 0.994), it decreases with intensity for the Emotion task (β_{emo} = −0.003; 95%CrI = [−0.005, −0.001]; $pp_{(\beta\ emo>0)}$ = 0.005), as further confirmed by a credible posterior difference between these two effects ($\beta_{col-emo}$ = 0.006; 95%CrI = [0.003, 0.009]; $pp_{(\beta\ col-emo>0)}$ = 1).

Neural encoding of emotion and color intensity

To reach a comprehensive understanding of whether threat expressions are prioritized during decision-making, we then tested Hypothesis 1 of an earlier selective neural encoding of threat-related information during the emotion task compared to the neural encoding of the color dimension in the color task. Instead of computing event-related averages, our EEG analyses consisted of a parametric regression-based approach where single-trial EEG signals were regressed against variables of interest (here the evidence strength, corresponding to the intensity of the displayed emotion or of the color mask) at each electrode and time point following the presentation of the stimulus. The resulting time course at each electrode represents the degree to which EEG activity 'encodes' (co-varies with) the evidence strength. Note that we first conducted this analysis separately for the emotion task (regressor: emotion intensity) and the color task (regressor: color intensity) and performed a multiple comparison correction on one-sample t-tests comparing parameter estimates against zero (null effect), to isolate the electrodes and timepoints where neural encoding of intensity was significant.

As illustrated in Figure 3A and Table 1, emotion intensity was encoded as soon as 100-200 ms over frontal and central electrodes in the emotion task, whereas the earliest cluster that encoded the color intensity in the color task did not appear until 260 ms over parietal and frontal electrodes (see Figure 3B). Five other clusters were found significant in the color task, which emerged at 370 ms, 490 ms and 660 ms (see Table 1 for full details).

We then conducted a multiple comparison analysis on the difference between the parameter estimates for emotion encoding and color encoding, which again revealed a significant cluster for the emotion intensity encoding between 100 ms and 230 ms. In contrast, only two of the six clusters identified in the first analysis were found to be significant when comparing emotion and color encoding directly, at 370 ms and 660 ms (see Table 1). In conclusion, there is a specific early encoding of emotion intensity around 100 ms, whereas there is a later encoding of color information starting at 270 ms.
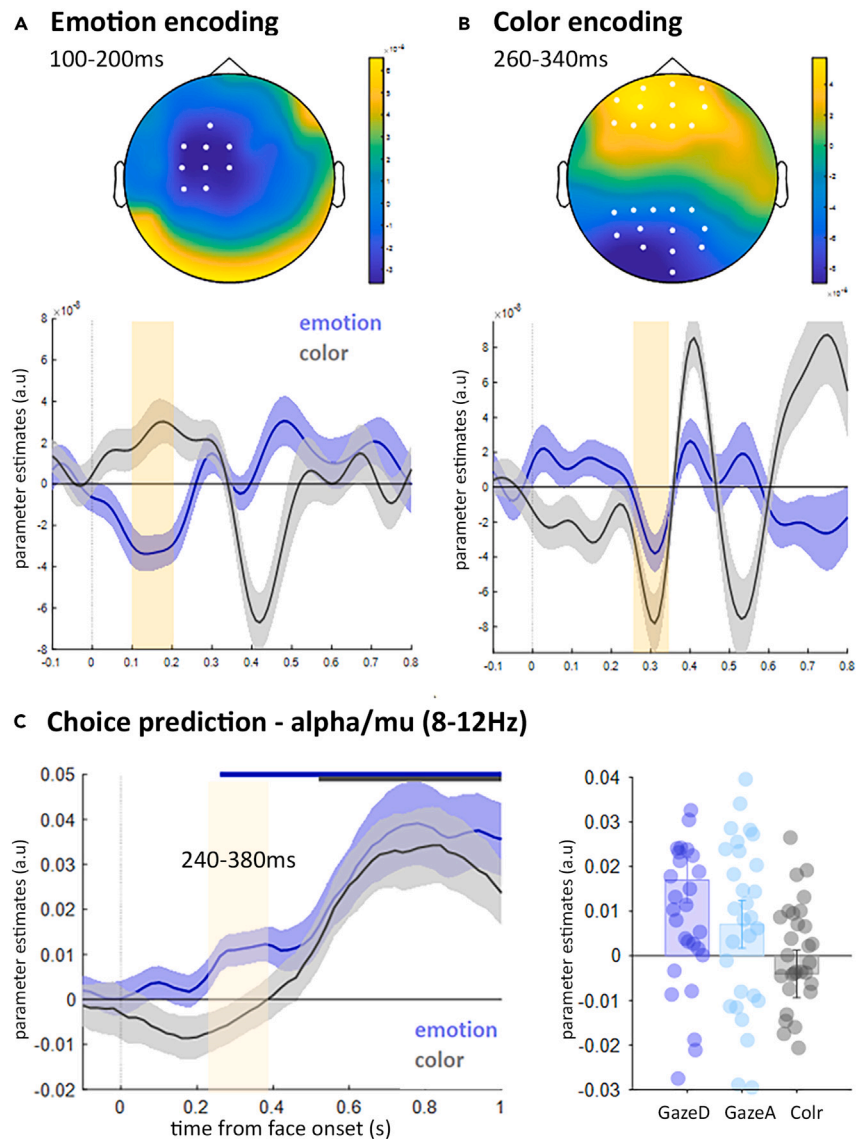
Figure 3. Neural encoding and choice-predictive activity

(A) Scalp topography of the first significant cluster for the encoding of emotion intensity (against zero), that emerged as soon as 100-200 ms on frontal and central electrodes. Significant electrodes are highlighted in white. A similar significant cluster was found when emotion encoding was contrasted to color encoding (see Table 1). Below the scalp topography, encoding time course for emotion (blue) and color (grey) decisions separately, expressed as mean parameter estimates in arbitrary units (a.u.) at electrodes of interest. Shaded error bars indicate s.e.m. Shaded light yellow area indicates the significant cluster time window (100-200 ms).

(B) Scalp topography of the first significant cluster for the encoding of color intensity (against zero), that appeared at 260 ms on parietal and frontal electrodes. Same conventions as (a).

(C) Time course of choice-predictive activity (stimulus-locked) in the motor lateralization index for emotion and color decisions in mu frequency band (8-12 Hz). Note that the motor-preparatory EEG signals were predictive of participants choices from 240 ms after stimulus onset during emotion decisions, and only from 520 ms following stimulus presentation during color decisions. Thick blue and grey lines at the top of the figure indicate the times where the parameter estimate is significant against zero (blue emotion task, grey color task). Shaded light yellow area indicates the timepoints where there is a significant difference between the two (240 ms–380 ms). The right panel shows the extracted parameter estimates averaged across the motor lateralization electrodes over the 240-380 ms window, separately for faces with direct (GazeD) and averted (GazeA) gaze for emotion decisions, as well as for color decision (Colr).

Choice prediction in the emotion vs. color task

Besides prioritized visual processing, we also hypothesized (H2) that the perception of threat-related facial displays would facilitate selection among action opportunities[60,61] promoting earlier preparation of the upcoming response in effector-selective structures.[16–22,41] Knowing that the suppression of mu-beta activity is a marker of motor preparation, we computed spectral power in the 8-12 Hz mu-alpha and 12-32 Hz

Table 1. Significant clusters for the encoding of emotion and color evidence

Time window	T statistic	p value	Electrodes
Emotion encoding against zero			
100-200ms	−164.24	0.0253	F1, FC3, FC1, C1, C3, CP3, CP1, FCz, Cz
Color encoding against zero			
260-340ms	−306.16	0.004	P1, P3, P5, P9, PO7, PO3, O1, Iz, Oz, POz, Pz, P2, PO4, O2
290-330ms	161.22	0.028	Fp1, AF7, AF3, F1, F3, F5, Fpz, Fp2, AF4, AFz, Fz, F2
370-450ms	−306.16	0.004	F1, FC3, FC1, C1, CPz, Fz, F2, F4, FC4, FC2, FCz, Cz, C2, C4
370-450ms	422.76	0.0013	P5, P7, P9, PO7, PO3, O1, Iz, Oz, POz, P8, P10, PO8
490-560ms	−181.56	0.0293	P1, P3, PO3, POz, Pz, P2, P4, P6, PO4
660-800ms	−142.44	0.0426	F6, F8, FT8, FC6, C6, T8
660-800ms	422.76	0.01	CP3, CP1, P1, P3, P5, PO3, O1, POz, Pz, CPz, CP4, CP2, PO4
Emotion vs. color			
100-230ms	−430.50	0.0013	F1, F3, FC1, C1, C3, CP3, CP1, CPz, Fz, F2, FC4, FCz, Cz, C2, CP2
90-210ms	257.90	0.005	P7, P9, PO7, O1, Iz, Oz, P10, PO8, O2
390-450ms	−208.34	0.01	P7, P9, PO7, O1, Iz, Oz, P10, PO8, O2
380-560ms	642.47	0.002	F1, FC1, C1, CP3, CP1, P1, P3, P5, PO3, Pz, CPz, Fz, F2, FC2, FCz, Cz, C2, C4, CP2, P2, P4, P6, PO4
620-800ms	−272.15	0.005	P1, PO3, Iz, Oz, POz, Pz, CP4, CP2, P4, P6, PO4, O2

mu-beta frequency bands to measure response-preparatory signals in the neural data.[31,62] For emotion/color decisions, we obtained the motor lateralization activity specific to 'anger'/'violet' responses by subtracting contralateral from ipsilateral mu spectral activity (8-12 Hz or 12-32 Hz) relative to the hand assigned to 'anger'/'violet' responses (counterbalanced across subjects), over effector-selective electrodes at each time point for all subjects. Then, to test Hypothesis 2 of an earlier prediction of the choice in motor-related signals during the emotion vs. the color task, we performed a logistic regression to predict the choice of Anger or Violet in the Emotion and Color tasks, respectively, with the motor lateralization activity in the 8-12 Hz mu-alpha band, and reaction times as an additional regressor. As shown in Figure 3C, the anger response was significantly predicted as soon as 260 ms (t-test against zero, $p < 0.05$), while the violet response was predicted at 520 ms, both up to 1s after stimulus onset (significant difference between the two tasks from 240 ms to 380 ms at $p < 0.05$, cluster-corrected p-value<0.001, Figure 3C; see also supplemental information: Figure S4 for the AUC values of the logistic model). We then performed the same analysis with the motor lateralization activity in the 12-32 Hz mu-beta band, but there were no differences in choice prediction between the two tasks (all $p > 0.08$). The prediction of choice by the 12-32 Hz mu-beta band was significant for both the anger response and the violet response around 420 ms after stimulus onset (starting at 420 ms for the emotion task, and at 440 ms for the color task, $p < 0.05$).

High threat signals influence on encoding and choice prediction

Finally, contextual cues, such as gaze or body direction, have been shown to significantly influence the judged relevance of the threat signals to the observer and the associated neural processing.[17,22,41] Our third hypothesis therefore predicted that both the encoding (H3a, Hypothesis 1 with the gaze direction) and the choice prediction (H3b, Hypothesis 2 with the gaze direction) should be stronger for high vs. low threat signals, i.e., for angry faces associated with direct gaze vs. averted gaze. To test whether gaze direction influenced emotion processing (H3a), we ran a cluster analysis on the encoding of emotion associated with direct and averted gaze separately, and then a direct comparison of the two. Only close to significance effects emerged for direct gaze emotion encoding (see Table 2), suggesting that the effects may be more important for high threat signals (although no significant differences between direct and averted gaze were observed).

To test whether choice prediction was stronger for angry faces with a direct gaze, we predicted the response 'anger' with the motor lateralization activity in the 8–12 Hz mu-alpha band in the previously isolated time window from 240 ms to 380 ms, separately for direct and averted gaze. As illustrated by Figure 3C, we found that only the choice prediction for faces with a direct gaze was significant against zero ($T36 = 3.52$, $p = 0.001$), while it was not significant for faces with an averted gaze and for the color choice ($p > 0.17$). There was a significant difference between the emotion choice prediction when the face had a direct gaze as compared to the color choice prediction ($T36 = 3.37$, $p = 0.0018$), but there were no significant differences between choice prediction for direct vs. averted gaze, nor for averted gaze vs. color ($p > 0.10$).

DISCUSSION

The present study investigated whether perceptual decisions about the emotional, threat-related aspects of stimuli engage specific or similar neural computations compared to decisions on their neutral, non-threatening components. We used electroencephalography (EEG) to simultaneously record brain activity, while participants performed two different detection tasks (emotion or color) on the same, two-dimensional

Table 2. Significant clusters for the encoding of emotional expressions with direct and averted gaze

Time window	T statistic	p value	Electrodes
Direct gaze emotion against zero			
80-130ms	−114.65	0.0706	F1, FC3, FC1, C1, C3, Fz, F2, FCz
270-330ms	152.96	0.03	AF3, F1, F3, Fpz, AF4, AFz, Fz, F2
270-320ms	−129.05	0.056	P5, P9, PO7, PO3, O1, Oz, P8, P10, PO8, PO4, O2
Averted gaze emotion against zero			
None		p > 0.9	
Direct vs. averted gaze emotion			
None		p > 0.6	

visual stimuli. Detection sensitivity was equalized across dimensions using an adaptive titration procedure. Our results revealed three specific effects when perceptual decisions concerned emotion rather than color. First, the amount of perceptual evidence (intensity) was encoded earlier (100–200 ms) in a cluster of central electrodes in the emotion task compared to the color task (290–330 ms). Second, participants' choices were predicted earlier by the mu-alpha EEG rhythm in the emotion task (240 ms) than in the color task (380 ms). Third, this choice-predictive activity over motor cortex was stronger for high-threat signals, i.e., for angry faces with direct versus averted gaze. Taken together, these findings indicate that perceptual decisions regarding the threat-signaling dimension of facial displays are associated with prioritized neural coding in action-related brain regions, supporting the motivational value of threat-related social signals.

Encoding of emotion and color intensity

Consistent with previous findings that threatening facial expressions receive privileged processing compared to neutral expressions and non-social stimuli[6] we observed earlier (100-200 ms) encoding of evidence strength in the emotion task compared to the color task (290-330 ms). Past experiments have shown that electrophysiological (MEG or EEG) activity discriminates emotional (anger) expressions from neutral expressions in the first 100 ms[39,63] and correlates with BOLD responses in the amygdala and occipital cortices.[64] Moreover, in contrast to gender or identity tasks, which are restricted to occipital regions, early emotion decoding (110-210 ms) involved a widely distributed network, including both temporo-parietal and frontal regions.[65] Together, these studies show that emotional, and particularly threatening, facial expressions are processed rapidly (from around 100 ms) by both subcortical and cortical brain networks. Here, by contrasting two perceptual decision tasks (emotion and color) performed on the same two-dimensional visual stimuli, we show that privileged processing in such an early time window (100-200 ms) benefits only the emotional, threat-signaling dimension.

Several authors have argued that perceptual saliency (including low-level perceptual features) and appraisal relevance jointly drive prioritized stimulus processing.[60,66–68] In the present study, owing to a titration procedure that equalized detection sensitivity across dimensions, highly salient information in the stimuli (angry expressions) did not interfere with the processing of color information during color decisions (see Figure 2A). Prioritization of the emotional, threat-related dimension may thus only occur when this information was relevant to the task at hand (i.e., during emotion decisions, not color decisions, see also[69]), concurring the suggestion that relevance detection is not automatic, but depends on task demands such as perceptual and/or cognitive load.[67] Besides being task-relevant, the emotional, threat-related dimension also varies in terms of its immediate relevance to the observer. Indeed, angry faces associated with direct or averted gaze clearly differ in terms of implied threat to the observer and have been shown to be appraised as high or low threat, respectively[53–55] Surprisingly, and contrary to our hypothesis based on previous findings,[41] no significant difference was observed between direct and averted angry faces in their early perceptual processing in the present study. Only near-significant effects were found for direct gaze emotion encoding. Note that this absence of significant difference between direct and averted angry displays may be related to a lack of statistical power, as only half of the trials were presented as compared to El Zein et al.,[41] as far as the effect of gaze is concerned.

Choice prediction

Additionally, and similar to past experiments that observed a buildup of choice-selective activity over motor-related regions during perceptual decision on non-social stimuli,[31,32,36,62,70–73] it was possible to statistically predict participants' choices from the mu/alpha power over motor cortical areas. This signal has been suggested to reflect the formation of an upcoming decision, i.e., a commitment to one choice alternative.[31,33,74] Here, we showed that the onset of choice predictive activity was earlier for emotion decisions (260 ms after stimulus onset) than for color decisions (520 ms), strongly suggesting that the emotional, threat-related dimension of our complex two-dimensional stimuli was not only processed, but also translated into action selection earlier than the color dimension. Moreover, this earlier choice predictive activity was stronger for high-threat signals, i.e., for angry faces with direct gaze compared to averted gaze.

The question remains as to why perceived social threats, notably those that are observer-relevant, lead to earlier selection between action opportunities in motor-related cortices. One likely explanation is related to the high behavioral/motivational relevance of emotional expressions. Evolutionary accounts of emotional displays argue that the very function of emotions is to serve communicative purposes by conveying critical information about the emitters[75–77] while also facilitating behavioral responses in the observers.[78,79] Emotional faces can be translated into action opportunities via different neural pathways (see review[61]). In humans, a growing body of literature concurs with evolutionary accounts by highlighting a functional and anatomical link between neural systems that sustain emotional appraisal and those that underlie action preparation.[21,80–82] Moreover, and in agreement with the present results, the influence of threat displays on motor-related areas was observed from 150 ms to 300 ms after stimulus onset.[16,17,20,41,57] We therefore propose that the earlier choice predictive activity during emotion decisions is related to the behavioral relevance of the perceived threat to the observer, rather than to its sensory properties. Threat-signaling emotions would facilitate the selection of adaptive behavioral responses.

Nevertheless, and somewhat counterintuitively, although participants' choices could be predicted earlier in the emotion task, their reaction times were longer than in the color task (even though we controlled for RTs in the choice predictive analysis). In the past, longer reaction times to emotional stimuli have been suggested to reflect an interference between the attentional resources devoted to their privileged processing and task demands.[83,84] Slower RTs to threatening stimuli could also reveal momentary freezing, which facilitates risk assessment by enhancing perceptual and attentional processes to the source of danger and preparing subsequent actions.[85,86] Here, we used drift-diffusion model analysis to show that the emotion task was associated with a smaller decrease in boundary separation with increasing intensity (a) and longer non-decision times (t0) compared to the color task. Consistent with our findings, the presentation of threat-related (fearful) facial expressions led participants to subsequently respond cautiously, as indexed by both slower reaction times and higher boundary separation, compared to neural expressions.[87] Moreover, higher boundary separation has also been found for emotional faces that have an immediate relevance to the observer,[88] i.e., fearful faces associated with averted gaze, which are rated as being both more intense [54,55] and more negative[89] compared to direct fearful faces. Beaurenaut et al.[88] proposed that participants are particularly cautious about misinterpreting such danger-related social signals. Furthermore, it has been shown that during perceptual decisions on non-social neutral stimuli, both higher boundary separation and larger non-decision time estimates are observed when participants are instructed to trade speed for accuracy.[90] Thus, in order to be more accurate, participants can increase their response caution, and/or adopt strategic motor slowing, i.e., delay their motor response once their decision has been made.[91] Even after the decision has been reached, longer t0 in response to threatening signals may suggest that a freezing mechanism is in place, involving motor execution speed. This interpretation seems consistent with the notion of freezing as a state of motor immobility, accompanied by heightened vigilance and caution.[92] Overall, this suggests that while perceptual decisions about threat-signaling emotions (relative to color) facilitate action selection among available alternatives, participants remain cautious and freeze before fully committing to and implementing the selected plan, to avoid costly misinterpretations.

Conclusion

In conclusion, this is the first study showing that the emotional, threat-related, dimension of our stimuli was processed and translated into motor activation earlier than the non-emotional (color) dimension, while equalizing the amount of sensory evidence, as well as participants' detection sensitivity, across tasks. Our findings strongly support the existence of prioritized neural computations for processing behaviorally and socially relevant signals, i.e., threat-related facial expressions, during perceptual decision-making. Earlier choice predictive activity over motor cortices during emotion decisions supports the idea that social threat displays are motivationally relevant, not only by providing information about others' affective states and potential behavioral intentions, but also by conveying action demands to the perceiver.[93]

Limitations of the study

The present experiment is not without limitations. First, our main results depend on the contrast with a control condition (color) that is neither social nor threatening, and thus cannot dissociate the processing of socio-emotional information from threat-related information in general. Yet, the contrast between direct and averted gaze allowed to provide some arguments in favor of threat prioritization, at least in terms of motor activation. Moreover, our experimental design allowed participants to perform two different detection tasks (emotion or color) on the same two-dimensional visual stimulus, while equalizing detection sensitivity across the two tasks. We propose that the prioritization of emotion decisions is driven by the interaction between the social nature of emotions and the behavioral relevance of anger. Still, we acknowledge that the absence of a significant difference between direct and averted angry faces in their early perceptual processing may be related to a lack of statistical power, suggesting that future studies should try to increase the number of trials to replicate both El Zein et al.[41] and the current results in a single study. Further work is also needed to complement the present findings, by contrasting social but non-threatening stimuli with non-social but threatening stimuli.

Second, although we equalized emotion and color decisions in terms of available sensory evidence and detection sensitivity, a difference in the reaction times and bias parameters was observed between the two types of decisions. To address this, we used single-trial regressions of EEG signals against the intensity of the displayed emotion and of the color mask, an experimental approach that measures stimulus sensitivity across tasks and which should dissociate perceptual and response bias. We also controlled all brain analyses on a trial-by-trial basis for the participants' subsequent detection reports (detection of violet in the color task, detection of anger in the emotion task). However, recent evidence in mice suggests that a lack of change in sensitivity does not prevent effects on sensory encoding – and that a behavioral bias can reveal such an effect.[94] Therefore, we cannot completely exclude that the observed privileged processing in the early time window

(100-200 ms), which only benefited the emotional, threat-signaling dimension during emotion decisions, may reflect a better sensory encoding of emotion compared to color.

STAR★METHODS

Detailed methods are provided in the online version of this paper and include the following:

- KEY RESOURCES TABLE
- RESOURCE AVAILABILITY
  - Lead contact
  - Materials availability
  - Data and code availability
- EXPERIMENTAL MODEL AND STUDY PARTICIPANT DETAILS
  - Participants
  - Stimuli
  - Experimental paradigm
  - Behavioral data analyses
  - Drift-diffusion models for behavioral data
  - EEG acquisition and pre-processing
  - EEG analyses

SUPPLEMENTAL INFORMATION

Supplemental information can be found online at https://doi.org/10.1016/j.isci.2024.109951.

AUTHOR CONTRIBUTIONS

Conceptualization: M.E.Z., V.W., and J.G.; Methodology: M.E.Z. and V.W.; Validation: M.E.Z.; Formal Analysis: M.E.Z., R.M., and M.S.; Investigation: M.E.Z. and E.M.; Data Curation: M.E.Z., R.M., V.W., and J.G.; Writing – Original Draft: M.E.Z., E.M., and J.G.; Writing – Review and Editing: M.E.Z., R.M., M.S., V.W., and J.G.; Visualization: M.E.Z., M.S., and J.G.; Supervision: V.W. and J.G.; Project Administration: V.W. and J.G.; Funding Acquisition: J.G.

DECLARATION OF INTERESTS

The authors declare no competing interests.

REFERENCES

1. Fletcher-Watson, S., Findlay, J.M., Leekam, S.R., and Benson, V. (2008). Rapid Detection of Person Information in a Naturalistic Scene. Perception 37, 571–583. https://doi.org/10.1068/p5705.

2. Ro, T., Russell, C., and Lavie, N. (2001). Changing Faces: A Detection Advantage in the Flicker Paradigm. Psychol. Sci. 12, 94–99. https://doi.org/10.1111/1467-9280.00317.

3. Bishop, H.J., Biasini, F.J., and Stavrinos, D. (2017). Social and Non-social Hazard Response in Drivers with Autism Spectrum Disorder. J. Autism Dev. Disord. 47, 905–917. https://doi.org/10.1007/s10803-016-2992-1.

4. Bannerman, R.L., Milders, M., and Sahraie, A. (2009). Processing emotional stimuli: Comparison of saccadic and manual choice-reaction times. Cogn. Emot. 23, 930–954. https://doi.org/10.1080/02699930802243303.

5. Schupp, H.T., Ohman, A., Junghöfer, M., Weike, A.I., Stockburger, J., and Hamm, A.O. (2004). The facilitated processing of threatening faces: an ERP analysis. Emotion 4, 189–200. https://doi.org/10.1037/1528-3542.4.2.189.

6. Vuilleumier, P. (2005). How brains beware: neural mechanisms of emotional attention. Trends Cogn. Sci. 9, 585–594. https://doi.org/10.1016/j.tics.2005.10.011.

7. Carretié, L. (2014). Exogenous (automatic) attention to emotional stimuli: a review. Cogn. Affect. Behav. Neurosci. 14, 1228–1258. https://doi.org/10.3758/s13415-014-0270-2.

8. Fox, E., and Damjanovic, L. (2006). The eyes are sufficient to produce a threat superiority effect. Emotion 6, 534–539. https://doi.org/10.1037/1528-3542.6.3.534.

9. Hansen, C.H., and Hansen, R.D. (1988). Finding the face in the crowd: An anger superiority effect. J. Pers. Soc. Psychol. 54, 917–924. https://doi.org/10.1037/0022-3514.54.6.917.

10. Pourtois, G., Schettino, A., and Vuilleumier, P. (2013). Brain mechanisms for emotional

influences on perception and attention: What is magic and what is not. Biol. Psychol. *92*, 492–512. https://doi.org/10.1016/j.biopsycho.2012.02.007.

11. Tamietto, M., Geminiani, G., Genero, R., and de Gelder, B. (2007). Seeing Fearful Body Language Overcomes Attentional Deficits in Patients with Neglect. J. Cogn. Neurosci. *19*, 445–454. https://doi.org/10.1162/jocn.2007.19.3.445.

12. Barbot, A., and Carrasco, M. (2018). Emotion and anxiety potentiate the way attention alters visual appearance. Sci. Rep. *8*, 5938. https://doi.org/10.1038/s41598-018-23686-8.

13. Becker, M.W. (2009). Panic Search: Fear Produces Efficient Visual Search for Nonthreatening Objects. Psychol. Sci. *20*, 435–437. https://doi.org/10.1111/j.1467-9280.2009.02303.x.

14. Chadwick, M., Metzler, H., Tijus, C., Armony, J.L., and Grèzes, J. (2019). Stimulus and observer characteristics jointly determine the relevance of threatening facial expressions and their interaction with attention. Motiv. Emot. *43*, 299–312. https://doi.org/10.1007/s11031-018-9730-2.

15. Phelps, E.A., Ling, S., and Carrasco, M. (2006). Emotion Facilitates Perception and Potentiates the Perceptual Benefits of Attention. Psychol. Sci. *17*, 292–299.

16. Borgomaneri, S., Vitale, F., and Avenanti, A. (2015). Early changes in corticospinal excitability when seeing fearful body expressions. Sci. Rep. *5*, 14122. https://doi.org/10.1038/srep14122.

17. Conty, L., Dezecache, G., Hugueville, L., and Grèzes, J. (2012). Early Binding of Gaze, Gesture, and Emotion: Neural Time Course and Correlates. J. Neurosci. *32*, 4531–4539. https://doi.org/10.1523/JNEUROSCI.5636-11.2012.

18. Grèzes, J., Pichon, S., and de Gelder, B. (2007). Perceiving fear in dynamic body expressions. Neuroimage *35*, 959–967. https://doi.org/10.1016/j.neuroimage.2006.11.030.

19. Hadjikhani, N., Hoge, R., Snyder, J., and de Gelder, B. (2008). Pointing with the eyes: The role of gaze in communicating danger. Brain Cogn. *68*, 1–8. https://doi.org/10.1016/j.bandc.2008.01.008.

20. Hortensius, R., de Gelder, B., and Schutter, D.J.L.G. (2016). When anger dominates the mind: Increased motor corticospinal excitability in the face of threat. Psychophysiology *53*, 1307–1316. https://doi.org/10.1111/psyp.12685.

21. Pichon, S., de Gelder, B., and Grèzes, J. (2012). Threat Prompts Defensive Brain Responses Independently of Attentional Control. Cereb. Cortex *22*, 274–285. https://doi.org/10.1093/cercor/bhr060.

22. Lima Portugal, L.C., Alves, R.d.C.S., Junior, O.F., Sanchez, T.A., Mocaiber, I., Volchan, E., Smith Erthal, F., David, I.A., Kim, J., Oliveira, L., et al. (2020). Interactions between emotion and action in the brain. Neuroimage *214*, 116728. https://doi.org/10.1016/j.neuroimage.2020.116728.

23. Mennella, R., Vilarem, E., and Grèzes, J. (2020). Rapid approach-avoidance responses to emotional displays reflect value-based decisions: Neural evidence from an EEG study. Neuroimage *222*, 117253. https://doi.org/10.1016/j.neuroimage.2020.117253.

24. Vilarem, E., Armony, J.L., and Grèzes, J. (2020). Action opportunities modulate attention allocation under social threat. Emotion *20*, 890–903. https://doi.org/10.1037/emo0000598.

25. Mennella, R., Bavard, S., Mentec, I., and Grèzes, J. (2022). Spontaneous instrumental avoidance learning in social contexts. Sci. Rep. *12*, 17528. https://doi.org/10.1038/s41598-022-22334-6.

26. Grèzes, J., Erblang, M., Vilarem, E., Quiquempoix, M., Van Beers, P., Guillard, M., Sauvet, F., Mennella, R., and Rabat, A. (2021). Impact of total sleep deprivation and related mood changes on approach-avoidance decisions to threat-related facial displays. Sleep *44*, zsab186. https://doi.org/10.1093/sleep/zsab186.

27. Grèzes, J., Risch, N., Courtet, P., Olié, E., and Mennella, R. (2023). Depression and approach-avoidance decisions to emotional displays: The role of anhedonia. Behav. Res. Ther. *164*, 104306. https://doi.org/10.1016/j.brat.2023.104306.

28. Kelly, S.P., and O'Connell, R.G. (2013). Internal and External Influences on the Rate of Sensory Evidence Accumulation in the Human Brain. J. Neurosci. *33*, 19434–19441. https://doi.org/10.1523/JNEUROSCI.3355-13.2013.

29. Steinemann, N.A., O'Connell, R.G., and Kelly, S.P. (2018). Decisions are expedited through multiple neural adjustments spanning the sensorimotor hierarchy. Nat. Commun. *9*, 3627. https://doi.org/10.1038/s41467-018-06117-0.

30. D'Andrea, A., Basti, A., Tosoni, A., Guidotti, R., Chella, F., Michelmann, S., Romani, G.L., Pizzella, V., and Marzetti, L. (2022). Magnetoencephalographic spectral fingerprints differentiate evidence accumulation from saccadic motor preparation in perceptual decision-making. iScience *25*, 105246. https://doi.org/10.1016/j.isci.2022.105246.

31. Donner, T.H., Siegel, M., Fries, P., and Engel, A.K. (2009). Buildup of Choice-Predictive Activity in Human Motor Cortex during Perceptual Decision Making. Curr. Biol. *19*, 1581–1585. https://doi.org/10.1016/j.cub.2009.07.066.

32. Gould, I.C., Nobre, A.C., Wyart, V., and Rushworth, M.F.S. (2012). Effects of Decision Variables and Intraparietal Stimulation on Sensorimotor Oscillatory Activity in the Human Brain. J. Neurosci. *32*, 13805–13818. https://doi.org/10.1523/JNEUROSCI.2200-12.2012.

33. Murphy, P.R., Boonstra, E., and Nieuwenhuis, S. (2016). Global gain modulation generates time-dependent urgency during perceptual choice in humans. Nat. Commun. *7*, 13526. https://doi.org/10.1038/ncomms13526.

34. O'Connell, R.G., Dockree, P.M., and Kelly, S.P. (2012). A supramodal accumulation-to-bound signal that determines perceptual decisions in humans. Nat. Neurosci. *15*, 1729–1735. https://doi.org/10.1038/nn.3248.

35. Twomey, D.M., Kelly, S.P., and O'Connell, R.G. (2016). Abstract and Effector-Selective Decision Signals Exhibit Qualitatively Distinct Dynamics before Delayed Perceptual Reports. J. Neurosci. *36*, 7346–7352. https://doi.org/10.1523/JNEUROSCI.4162-15.2016.

36. Wyart, V., de Gardelle, V., Scholl, J., and Summerfield, C. (2012). Rhythmic fluctuations in evidence accumulation during decision making in the human brain. Neuron *76*, 847–858. https://doi.org/10.1016/j.neuron.2012.09.015.

37. Yau, Y., Dadar, M., Taylor, M., Zeighami, Y., Fellows, L.K., Cisek, P., and Dagher, A. (2020). Neural Correlates of Evidence and Urgency During Human Perceptual Decision-Making in Dynamically Changing Conditions. Cereb. Cortex, 5471–5483. https://doi.org/10.1093/cercor/bhaa129.

38. Yau, Y., Hinault, T., Taylor, M., Cisek, P., Fellows, L.K., and Dagher, A. (2021). Evidence and Urgency Related EEG Signals during Dynamic Decision-Making in Humans. J. Neurosci. *41*, 5711–5722. https://doi.org/10.1523/JNEUROSCI.2551-20.2021.

39. Kaminska, O.K., Magnuski, M., Olszanowski, M., Gola, M., Brzezicka, A., and Winkielman, P. (2020). Ambiguous at the second sight: Mixed facial expressions trigger late electrophysiological responses linked to lower social impressions. Cogn. Affect. Behav. Neurosci. *20*, 441–454. https://doi.org/10.3758/s13415-020-00778-5.

40. Dricu, M., and Frühholz, S. (2020). A neurocognitive model of perceptual decision-making on emotional signals. Hum. Brain Mapp. *41*, 1532–1556. https://doi.org/10.1002/hbm.24893.

41. El Zein, M., Wyart, V., and Grèzes, J. (2015). Anxiety dissociates the adaptive functions of sensory and motor response enhancements to social threats. Elife *4*, e10274. https://doi.org/10.7554/eLife.10274.

42. Pessoa, L., and Padmala, S. (2005). Quantitative prediction of perceptual decisions during near-threshold fear detection. Proc. Natl. Acad. Sci. USA *102*, 5612–5617. https://doi.org/10.1073/pnas.0500566102.

43. Pessoa, L., and Padmala, S. (2007). Decoding Near-Threshold Perception of Fear from Distributed Single-Trial Brain Activation. Cereb. Cortex *17*, 691–701. https://doi.org/10.1093/cercor/bhk020.

44. Thielscher, A., and Pessoa, L. (2007). Neural Correlates of Perceptual Choice and Decision Making during Fear–Disgust Discrimination. J. Neurosci. *27*, 2908–2917. https://doi.org/10.1523/JNEUROSCI.3024-06.2007.

45. Arabadzhiyska, D.H., Garrod, O.G.B., Fouragnan, E., De Luca, E., Schyns, P.G., and Philiastides, M.G. (2022). A Common Neural Account for Social and Nonsocial Decisions. J. Neurosci. *42*, 9030–9044. https://doi.org/10.1523/JNEUROSCI.0375-22.2022.

46. Delis, I., Onken, A., Schyns, P.G., Panzeri, S., and Philiastides, M.G. (2016). Space-by-time decomposition for single-trial decoding of M/EEG activity. Neuroimage *133*, 504–515. https://doi.org/10.1016/j.neuroimage.2016.03.043.

47. Heekeren, H.R., Marrett, S., Bandettini, P.A., and Ungerleider, L.G. (2004). A general mechanism for perceptual decision-making in the human brain. Nature *431*, 859–862. https://doi.org/10.1038/nature02966.

48. Philiastides, M.G., Ratcliff, R., and Sajda, P. (2006). Neural Representation of Task Difficulty and Decision Making during Perceptual Categorization: A Timing Diagram. J. Neurosci. *26*, 8965–8975. https://doi.org/10.1523/JNEUROSCI.1655-06.2006.

49. Philiastides, M.G., and Sajda, P. (2006). Temporal Characterization of the Neural

Correlates of Perceptual Decision Making in the Human Brain. Cereb. Cortex 16, 509–518. https://doi.org/10.1093/cercor/bhi130.

50. Philiastides, M.G., and Sajda, P. (2007). EEG-Informed fMRI Reveals Spatiotemporal Characteristics of Perceptual Decision Making. J. Neurosci. 27, 13082–13091. https://doi.org/10.1523/JNEUROSCI.3540-07.2007.

51. Tu, T., Schneck, N., Muraskin, J., and Sajda, P. (2017). Network Configurations in the Human Brain Reflect Choice Bias during Rapid Face Processing. J. Neurosci. 37, 12226–12237. https://doi.org/10.1523/JNEUROSCI.1677-17.2017.

52. Sun, S., Yu, R., and Wang, S. (2017). A Neural Signature Encoding Decisions under Perceptual Ambiguity. eNeuro 4. ENEURO. 0235-17.2017. https://doi.org/10.1523/ENEURO.0235-17.2017.

53. Adams, R.B., and Kleck, R.E. (2003). Perceived gaze direction and the processing of facial displays of emotion. Psychol. Sci. 14, 644–647. https://doi.org/10.1046/j.0956-7976.2003.psci_1479.x.

54. Cristinzio, C., N'Diaye, K., Seeck, M., Vuilleumier, P., and Sander, D. (2010). Integration of gaze direction and facial expression in patients with unilateral amygdala damage. Brain 133, 248–261. https://doi.org/10.1093/brain/awp255.

55. N'Diaye, K., Sander, D., and Vuilleumier, P. (2009). Self-relevance processing in the human amygdala: Gaze direction, facial expression, and emotion intensity. Emotion 9, 798–806.

56. Stussi, Y., Brosch, T., and Sander, D. (2015). Learning to fear depends on emotion and gaze interaction: The role of self-relevance in fear learning. Biol. Psychol. 109, 232–238. https://doi.org/10.1016/j.biopsycho.2015.06.008.

57. El Zein, M., Gamond, L., Conty, L., and Grèzes, J. (2015). Selective attention effects on early integration of social signals: same timing, modulated neural sources. Neuroimage 106, 182–188. https://doi.org/10.1016/j.neuroimage.2014.10.063.

58. Guex, R., Meaux, E., Mégevand, P., Domínguez-Borràs, J., Seeck, M., and Vuilleumier, P. (2023). Frequency-specific gaze modulation of emotional face processing in the human amygdala. Cereb. Cortex 33, 4859–4869. https://doi.org/10.1093/cercor/bhac385.

59. Ratcliff, R., and McKoon, G. (2008). The diffusion decision model: theory and data for two-choice decision tasks. Neural Comput. 20, 873–922. https://doi.org/10.1162/neco.2008.12-06-420.

60. Frijda, N.H. (2009). Emotion experience and its varieties. Emot. Rev. 1, 264–271. https://doi.org/10.1177/1754073909103595.

61. Mennella, R., and Grezes, J. (2023). How Emotional Expressions Motivate Action. PsyArXiv. https://doi.org/10.31234/osf.io/vfbcp.

62. de Lange, F.P., Rahnev, D.A., Donner, T.H., and Lau, H. (2013). Prestimulus oscillatory activity over motor cortex reflects perceptual expectations. J. Neurosci. 33, 1400–1410. https://doi.org/10.1523/JNEUROSCI.1094-12.2013.

63. Dima, D.C., Perry, G., Messaritaki, E., Zhang, J., and Singh, K.D. (2018). Spatiotemporal dynamics in human visual cortex rapidly encode the emotional content of faces.

Hum. Brain Mapp. 39, 3993–4006. https://doi.org/10.1002/hbm.24226.

64. Müller-Bardorff, M., Bruchmann, M., Mothes-Lasch, M., Zwitserlood, P., Schlossmacher, I., Hofmann, D., Miltner, W., and Straube, T. (2018). Early brain responses to affective faces: A simultaneous EEG-fMRI study. Neuroimage 178, 660–667. https://doi.org/10.1016/j.neuroimage.2018.05.081.

65. Li, Y., Zhang, M., Liu, S., and Luo, W. (2022). EEG decoding of multidimensional information from emotional faces. Neuroimage 258, 119374. https://doi.org/10.1016/j.neuroimage.2022.119374.

66. Brosch, T., Pourtois, G., and Sander, D. (2010). The perception and categorisation of emotional stimuli: A review. Cogn. Emot. 24, 377–400. https://doi.org/10.1080/02699930902975754.

67. Maratos, F.A., and Pessoa, L. (2019). What drives prioritized visual processing? A motivational relevance account. Prog. Brain Res. 247, 111–148. https://doi.org/10.1016/bs.pbr.2019.03.028.

68. Sander, D., Grafman, J., and Zalla, T. (2003). The human amygdala: an evolved system for relevance detection. Rev. Neurosci. 14, 303–316. https://doi.org/10.1515/revneuro.2003.14.4.303.

69. Mirabella, G. (2018). The Weight of Emotions in Decision-Making: How Fearful and Happy Facial Stimuli Modulate Action Readiness of Goal-Directed Actions. Front. Psychol. 9, 1334. https://doi.org/10.3389/fpsyg.2018.01334.

70. Alamia, A., Zénon, A., VanRullen, R., Duque, J., and Derosiere, G. (2019). Implicit visual cues tune oscillatory motor activity during decision-making. Neuroimage 186, 424–436. https://doi.org/10.1016/j.neuroimage.2018.11.027.

71. Chandrasekaran, C., Bray, I.E., and Shenoy, K.V. (2019). Frequency Shifts and Depth Dependence of Premotor Beta Band Activity during Perceptual Decision-Making. J. Neurosci. 39, 1420–1435. https://doi.org/10.1523/JNEUROSCI.1066-18.2018.

72. Derosiere, G., Thura, D., Cisek, P., and Duque, J. (2019). Motor cortex disruption delays motor processes but not deliberation about action choices. J. Neurophysiol. 122, 1566–1577. https://doi.org/10.1152/jn.00163.2019.

73. Tosoni, A., Corbetta, M., Calluso, C., Committeri, G., Pezzulo, G., Romani, G.L., and Galati, G. (2014). Decision and action planning signals in human posterior parietal cortex during delayed perceptual choices. Eur. J. Neurosci. 39, 1370–1383. https://doi.org/10.1111/ejn.12511.

74. Rogge, J., Jocham, G., and Ullsperger, M. (2022). Motor cortical signals reflecting decision making and action preparation. Neuroimage 263, 119667. https://doi.org/10.1016/j.neuroimage.2022.119667.

75. Buck, R. (1994). Social and emotional functions in facial expression and communication: the readout hypothesis. Biol. Psychol. 38, 95–115. https://doi.org/10.1016/0301-0511(94)90032-9.

76. Parkinson, B. (2005). Do facial movements express emotions or communicate motives? Pers. Soc. Psychol. Rev. 9, 278–311. https://doi.org/10.1207/s15327957pspr0904_1.

77. Crivelli, C., and Fridlund, A.J. (2018). Facial Displays Are Tools for Social Influence. Trends Cogn. Sci. 22, 388–399. https://doi.org/10.1016/j.tics.2018.02.006.

78. Dezecache, G., Mercier, H., and Scott-Phillips, T.C. (2013). An evolutionary approach to emotional communication. J. Pragmat. 59, 221–233. https://doi.org/10.1016/j.pragma.2013.06.007.

79. Dezecache, G., Jacob, P., and Grèzes, J. (2015). Emotional contagion: its scope and limits. Trends Cogn. Sci. 19, 297–299. https://doi.org/10.1016/j.tics.2015.03.011.

80. de Gelder, B., Snyder, J., Greve, D., Gerard, G., and Hadjikhani, N. (2004). Fear fosters flight: a mechanism for fear contagion when perceiving emotion expressed by a whole body. Proc. Natl. Acad. Sci. USA 101, 16701–16706. https://doi.org/10.1073/pnas.0407042101.

81. Grèzes, J., Valabrègue, R., Gholipour, B., and Chevallier, C. (2014). A direct amygdala-motor pathway for emotional displays to influence action: A diffusion tensor imaging study. Hum. Brain Mapp. 35, 5974–5983. https://doi.org/10.1002/hbm.22598.

82. Van den Stock, J., Tamietto, M., Sorger, B., Pichon, S., Grézes, J., and de Gelder, B. (2011). Cortico-subcortical visual, somatosensory, and motor activations for perceiving dynamic whole-body emotional expressions with and without striate cortex (V1). Proc. Natl. Acad. Sci. USA 108, 16188–16193. https://doi.org/10.1073/pnas.1107214108.

83. Pessoa, L. (2009). How do emotion and motivation direct executive control? Trends Cogn. Sci. 13, 160–166. https://doi.org/10.1016/j.tics.2009.01.006.

84. Williams, J.M., Mathews, A., and MacLeod, C. (1996). The emotional Stroop task and psychopathology. Psychol. Bull. 120, 3–24. https://doi.org/10.1037/0033-2909.120.1.3.

85. Sagliano, L., Cappuccio, A., Trojano, L., and Conson, M. (2014). Approaching threats elicit a freeze-like response in humans. Neurosci. Lett. 561, 35–40. https://doi.org/10.1016/j.neulet.2013.12.038.

86. Sagliano, L., Vela, M., Trojano, L., and Conson, M. (2019). The role of the right premotor cortex and temporo-parietal junction in defensive responses to visual threats. Cortex 120, 532–538. https://doi.org/10.1016/j.cortex.2019.08.005.

87. Tipples, J. (2018). Caution follows fear: Evidence from hierarchical drift diffusion modelling. Emotion 18, 237–247. https://doi.org/10.1037/emo0000342.

88. Beaurenaut, M., Mennella, R., Dezecache, G., and Grèzes, J. (2023). Prioritization of danger-related social signals during threat-induced anxiety. Emotion 23, 2356–2369. https://doi.org/10.1037/emo0001231.

89. Ewbank, M.P., Fox, E., and Calder, A.J. (2010). The interaction between gaze and facial expression in the amygdala and extended amygdala is modulated by anxiety. Front. Hum. Neurosci. 4, 56. https://doi.org/10.3389/fnhum.2010.00056.

90. Voss, A., Rothermund, K., and Voss, J. (2004). Interpreting the parameters of the diffusion model: An empirical validation. Mem. Cognit. 32, 1206–1220. https://doi.org/10.3758/BF03196893.

91. White, C.N., Congdon, E., Mumford, J.A., Karlsgodt, K.H., Sabb, F.W., Freimer, N.B., London, E.D., Cannon, T.D., Bilder, R.M., and Poldrack, R.A. (2014). Decomposing Decision Components in the Stop-signal Task: A Model-based Approach to Individual Differences in Inhibitory Control.

J. Cogn. Neurosci. *26*, 1601–1614. https://doi.org/10.1162/jocn_a_00567.

92. Roelofs, K. (2017). Freeze for action: neurobiological mechanisms in animal and human freezing. Philos. Trans. R. Soc. Lond. B Biol. Sci. *372*, 20160206. https://doi.org/10.1098/rstb.2016.0206.

93. Horstmann, G. (2003). What do facial expressions convey: feeling states, behavioral intentions, or action requests? Emotion *3*, 150–166. https://doi.org/10.1037/1528-3542.3.2.150.

94. Jin, M., and Glickfeld, L.L. (2019). Contribution of Sensory Encoding to Measured Bias. J. Neurosci. *39*, 5115–5127. https://doi.org/10.1523/JNEUROSCI.0076-19.2019.

95. Langner, O., Dotsch, R., Bijlstra, G., Wigboldus, D.H.J., Hawk, S.T., and van Knippenberg, A. (2010). Presentation and validation of the Radboud Faces Database. Cogn. Emot. *24*, 1377–1388. https://doi.org/10.1080/02699930903485076.

96. Caruana, N., Inkley, C., and El Zein, M. (2020). Gaze direction biases emotion categorisation in schizophrenia. Schizophr. Res. Cogn. *21*, 100181. https://doi.org/10.1016/j.scog.2020.100181.

97. Ioannou, C., Zein, M.E., Wyart, V., Scheid, I., Amsellem, F., Delorme, R., Chevallier, C., and Grèzes, J. (2017). Shared mechanism for emotion processing in adolescents with and without autism. Sci. Rep. *7*, 42696. https://doi.org/10.1038/srep42696.

98. Brainard, D.H. (1997). The Psychophysics Toolbox. Spat. Vis. *10*, 433–436.

99. Pelli, D.G. (1997). The VideoToolbox software for visual psychophysics: transforming numbers into movies. Spat. Vis. *10*, 437–442.

100. Kaernbach, C. (1991). Simple adaptive testing with the weighted up-down method. Percept. Psychophys. *49*, 227–229. https://doi.org/10.3758/bf03214307.

101. Wiecki, T.V., Sofer, I., and Frank, M.J. (2013). HDDM: Hierarchical Bayesian estimation of the Drift-Diffusion Model in Python. Front. Neuroinform. *7*, 14.

102. Lerche, V., and Voss, A. (2016). Model Complexity in Diffusion Modeling: Benefits of Making the Model More Parsimonious. Front. Psychol. *7*, 1324.

103. Boehm, U., Annis, J., Frank, M.J., Hawkins, G.E., Heathcote, A., Kellen, D., Krypotos, A.-M., Lerche, V., Logan, G.D., Palmeri, T.J., et al. (2018). Estimating across-trial variability parameters of the Diffusion Decision Model: Expert advice and recommendations. J. Math. Psychol. *87*, 46–75. https://doi.org/10.1016/j.jmp.2018.09.004.

104. Dutilh, G., Annis, J., Brown, S.D., Cassey, P., Evans, N.J., Grasman, R.P.P.P., Hawkins, G.E., Heathcote, A., Holmes, W.R., Krypotos, A.-M., et al. (2019). The Quality of Response Time Data Inference: A Blinded, Collaborative Assessment of the Validity of Cognitive Models. Psychon. Bull. Rev. *26*, 1051–1069. https://doi.org/10.3758/s13423-017-1417-2.

105. Ando, T. (2007). Bayesian predictive information criterion for the evaluation of hierarchical Bayesian and empirical Bayes models. Biometrika *94*, 443–458. https://doi.org/10.1093/biomet/asm017.

106. Tadel, F., Baillet, S., Mosher, J.C., Pantazis, D., and Leahy, R.M. (2011). Brainstorm: a user-friendly application for MEG/EEG analysis. Comput. Intell. Neurosci. *2011*, 879716. https://doi.org/10.1155/2011/879716.

107. Wyart, V., Myers, N.E., and Summerfield, C. (2015). Neural mechanisms of human perceptual choice under focused and divided attention. J. Neurosci. *35*, 3485–3498. https://doi.org/10.1523/JNEUROSCI.3276-14.2015.

108. Oostenveld, R., Fries, P., Maris, E., and Schoffelen, J.-M. (2011). FieldTrip: Open Source Software for Advanced Analysis of MEG, EEG, and Invasive Electrophysiological Data. Comput. Intell. Neurosci. *2011*, e156869. https://doi.org/10.1155/2011/156869.

STAR★METHODS

KEY RESOURCES TABLE

REAGENT or RESOURCE	SOURCE	IDENTIFIER
Deposited data		
Behavior and EEG data	This paper	OSF or Zenodo: https://doi.org/xxxx
Software and algorithms		
MATLAB	The Mathworks, Natick, MA, USA	https://www.mathworks.com/products/matlab.html
Psychophysics-3 toolbox	free set of Matlab and GNU Octave functions for vision and neuroscience research.	http://psychtoolbox.org/
Python package HDDM	MATLAB software toolbox for MEG, EEG and iEEG analysis,	https://hddm.readthedocs.io/en/latest/index.html
Fieldtrip Toolbox	Open-source MATLAB software toolbox for MEG, EEG and iEEG analysis	https://www.fieldtriptoolbox.org/
Brainstorm Toolbox	Open-source application for MEG/EEG data analysis	https://github.com/brainstorm-tools/brainstorm3
R version 4.1.1	The R Project for Statistical Computing	https://www.r-project.org/

RESOURCE AVAILABILITY

Lead contact

Further information and requests for resources should be directed to and will be fulfilled by the lead contact, Julie Grèzes (julie.grezes@ens.psl.eu).

Materials availability

This study did not generate new unique reagents.

Data and code availability

De-identified EEG data and behavioral data have been deposited at the Open Science Framework (OSF) and will be publicly available, once the paper is accepted at https://osf.io/zmyaf/?view_only=93561733ef3f4d6e88fe50fea13d2e03.

All original codes have been at the Open Science Framework (OSF) and will be publicly available, once the paper is accepted at https://osf.io/zmyaf/?view_only=93561733ef3f4d6e88fe50fea13d2e03.

Any additional information required to reanalyse the data reported in this paper is available from the lead contact upon request.

EXPERIMENTAL MODEL AND STUDY PARTICIPANT DETAILS

Participants

Thirty-eight healthy young adults (20 females; mean age $\pm$s.d. = 23.15 $\pm$ 3.38 years) participated in an EEG experiment. All participants were right-handed, had normal vision and no neurological or psychiatric history. The experimental protocol was approved by INSERM and the local research ethics committee (Comité de protection des personnes Ile de France III - Project CO7-28, N° Eudract: 207-A01125-48) and was conducted in accordance with the Declaration of Helsinki. Participants provided written informed consent and were compensated for their participation. One participant was excluded from the analyses due to a technical error while saving the data, and analyses were performed on 37 participants (20 females, mean age = 23.16 $\pm$ 3.42 years).

Stimuli

The stimuli consisted of morphed facial emotion expressions ranging from neutral to angry expressions[41,95] that have been used in several studies.[41,57,96,97] The full description of the stimuli can be found in El Zein et al.,[41] and the stimuli are available upon request. 16 identities (8 females) were included in the current study. They varied in gaze direction (direct or averted 45° to the left or right) and emotion intensity - from neutral to angry expressions with 7 levels of emotion. In addition, we created color masks over the faces, morphed from gray to violet with 7 levels of violet. To calibrate the morphing between the emotional expressions and the color masks, we ran an intensity rating pre-test of the emotional and color morphs on an independent sample of participants (n = 10). Participants were presented with facial expressions or color masks for 250 ms and rated their perceived intensity on a continuous scale from "not at all intense" to "very intense" using a mouse device

(with a maximum of 3 s to respond). Based on the results, we adjusted for differences between emotion and color morphs by linearizing the mean curves of the judged intensities and creating corresponding morphs that were equalized according to the perceived intensities.

Experimental paradigm

Using the Psychophysics-3 toolbox,[98,99] stimuli were projected onto a black screen. Each trial began with a white oval delineating the faces that remained throughout the trial (see Figure 1). The white oval appeared for approximately 500 ms, followed by a white fixation dot presented at the eye level for approximately 1000 ms (to ensure a natural fixation on the upcoming faces and to avoid eye movements from the center of the oval to the eye region). Then, the morphed face, over which we superimposed a morphed color mask, was presented for 250 ms. After the face offset, participants had to make either an emotion or a color decision in a blocked design. Depending on the block, participants were asked to report (max. 2s after face offset) the presence or absence of either emotion (anger) or color (violet) in the stimulus, while ignoring the other task-irrelevant dimension (see Figure 1). They provided their response by pressing one of the two buttons 'Right Control' and 'Left Control' keys on the keyboard with their right and left index, respectively. A gray/violet and neutral/anger key mapping was used (4 possible hand mappings), kept constant within subjects and counterbalanced across subjects. The experiment was divided into 32 experimental blocks (16 blocks of emotion decisions, 16 blocks of color decisions), each consisting of 32 trials, balanced in the number of gaze directions (2), gender (2), and morph levels (8). Color masks and emotions were combined semi-randomly, such that within each block, no correlation between emotion and color intensity was allowed (r < 0.05, p > 0.6). This resulted in a total of 512 trials (32 trials*16 identities) per decision type (emotion/color), and 1024 trials for the entire experiment. Participants alternated between the emotion and color tasks at each block. Prior to the experiment, each participant completed a short practice session (one emotion and one color block, two identities, 16 trials each).

To ensure that the observed differences at the neural level between tasks did not depend on differences in detection sensitivity to emotion and color dimensions, we equalized detection sensitivity across emotion and color dimensions using an adaptive Bayesian titration procedure. Participants completed a short titration session of two blocks (one emotion and one color block, two identities, 32 trials each), and each participant's perceptual sensitivity to both emotion and color dimensions was estimated separately. The emotion or color morph level were entered as independent variables in a binomial general linear model (GLM) with probit link function to predict participants' choices, and parameter estimates were extracted for each dimension. These parameter estimates were then used to calculate a titration factor (i.e., multiplier) that was multiplied by the color mask morph applied to the face, allowing the color level of the stimulus to be rescaled to the same perceptual intensity as the emotion level.[100] This procedure was reiterated every two blocks throughout the experiment. This ensured that the detection sensitivity between emotion and color decisions was calibrated and updated across the experiment, so that the same slope of the psychometric function reflected participants' behavior in both conditions.

Participants were informed prior to the experiment that they would receive one point for each "correct" response (i.e., correct detection when the morph level was >3), which could result in a bonus of 5–10 Euros, depending on their final score. Feedback on their performance (i.e., percentage of correct responses) was displayed on the screen after each block. Every 8 blocks, a progress bar allowed participants to estimate how close they were to receiving a bonus. At the end of the experiment, all participants received the same compensation, regardless of their performance.

Behavioral data analyses

The theoretical framework of Signal Detection Theory distinguishes between sensitivity to sensory information and response bias (or criterion) that reflects the observer's tendency to interpret the face as displaying either one of the two options (anger or neutral for emotion decisions, violet or gray for color decisions). Within this framework, we used a model of choice hypothesizing that decisions are formed based on a noisy comparison between the displayed emotion or color and a criterion. For emotion and color decisions separately, we fitted the data with the simplest model (model 0) that could account for each subject's decisions using a noisy, 'signal detection'-like psychometric model, to which we included a lapse rate to account for random guessing:

$$P(anger) = \phi[\omega\_emo * x\_emo + b\_emo]*(1-\varepsilon)+\varepsilon$$

$$P(violet) = \phi[\omega\_colr * x\_colr + b\_colr]*(1-\varepsilon)+\varepsilon$$

where P(anger) and P(violet) correspond to the probability of judging the face as angry or violet, respectively, $\phi(.)$ to the cumulative normal function, ω_emo and ω_colr to the perceptual sensitivity to the displayed emotion or color, x_emo and x_colr to the a trial-wise array of evidence values in favor of anger (emotion intensity in the stimulus) or of violet (color intensity in the stimulus) (from 0 for neutral to +7 for an intense display), b_emo and b_colr to an additive, stimulus-independent bias toward one of the neutral/anger or gray/violet choices, and ε to the proportion of random guesses among the choices. Parameters were estimated by minimizing the model's negative log likelihood using the fmincon function in MATLAB. The bias parameter had an initial value of 0 and was constrained between −7 and +7; the sensitivity parameter had an initial value of 1 and was constrained between 0 and 10; the lapse rate parameter had an initial value of 0.2 and was constrained between 0 and 0.8. Sensitivity (ω_emo, ω_colr) and bias (b_emo, b_colr) parameters computed with these models were then compared using

t-test analyses. We also assessed "interference" effects between stimulus dimensions by examining whether the decision-irrelevant stimulus dimension (i.e., emotion intensity in color decisions, and color intensity in emotion decisions) influenced the processing of decision-relevant cues.

Drift-diffusion models for behavioral data

To better understand the difference in decision bias parameters and reaction times between the Emotion and the Color tasks (see behavioral results), we fitted DDMs choices and RTs distributions using the Python package HDDM.[101] HDDM implements a Bayesian hierarchical estimation of DDM parameters at the individual and group level using Markov Chain Monte Carlo (MCMC) sampling. To fit the models, responses were coded "Angry/Violet" responses and "Neutral/Gray" responses during the Emotion and Color tasks, respectively. The task (Emotion vs. Color), the continuous intensity level (centered, −3.5 to 3.5 in eight steps), and their interaction were fitted as regression parameters in the DDMs. To improve the interpretability of the parameter estimates, we adopted a cell design matrix estimating one parameter (a, v, z or t0) for each task, and the effect of intensity on each of them.

Eight models were run to understand the influence of task type and intensity level on decision. First, we ran 7 models to test the effect of task and intensity on drift rate (v), threshold (a), and non-decision time (t0) individually or in combination. In all these models, we estimated separate bias (z) parameters by task. Finally, we tested whether the best-fitting model in the first step of model selection was improved by removing the effect of task on the bias parameter. Due to the moderate number of trials per condition, we simplified the models in several ways: the boundaries of the model were associated with "Angry/Violet" (upper threshold) and "Neutral/Gray" responses (lower threshold), regardless of whether they required a left or right button press (correspondence was counterbalanced across participants, but stable within participants); furthermore, the inter-trial variabilities were fixed to zero, since a proper fit of these parameters is particularly challenging, especially with small to medium-sized trials number.[102–104]

Models were compared using their Deviance Information Criterion (DIC) and Bayesian Predictive Information Criterion (BPIC) values.[105] Further analyses were performed on the best-fitting model (i.e., lower DIC and BPIC). We based inference on the 95% credible intervals (95%CrI) of the group-level parameters, defined as the interval between the 2.5^{th} and 97.5^{th} quantiles of the estimates' posterior distributions (or the posterior distribution of the parameter differences when testing for them). We considered a parameter (or a difference) to be credible if the 95%CrI did not overlap with 0 (or 0.5 in the case of the starting point bias, i.e., a perfectly equidistant point between the two response boundaries). MCMC sampling was generated using 3 chains of 5000 iterations each (1500 of which were used as a burn-in period). Detailed information about model diagnostic can be found in supplementary text.

EEG acquisition and pre-processing

EEG was recorded continuously from 64 scalp sites with CMS/DRL reference electrodes using a BioSemi headcap with active electrodes. The EEG signal was amplified using an ActiveTwo AD-box amplifier (BioSemi), low-pass filtered online (250 Hz) and digitized at 1000 Hz. Raw EEG data were pre-processed using the Brainstorm toolbox for MATLAB.[106]

First, raw EEG was recalculated to average reference, down-sampled to 500 Hz (2 ms steps), and band-pass filtered between 1 and 40 Hz. Second, EEG data were visually inspected to remove muscle artifacts and to identify noisy electrodes, which were interpolated to the average of adjacent electrodes. Third, independent component analysis (ICA) excluding interpolated electrodes was performed on the continuous data and ICA components capturing eye blink artifacts were rejected. These EEG data were then epoched from 2s before to 2s after the face stimulus onset (20 ms steps) and linearly de-trended. Epochs containing activity exceeding a threshold of +/− 70 μV were automatically discarded. Finally, the resulting individual epochs were visually inspected to manually exclude any remaining trials with artifacts. After trial rejection, the remaining trials averaged 975 ± 46 trials per subject. The resulting data were resampled to 100 Hz (10 ms steps) from 500 ms before to 1.5s after stimulus onset.

Time-frequency decomposition was also performed using a Brainstorm Toolbox pipeline. Time-frequency representations (TFRs) of individual trials were computed for each subject. The Morlet Wavelet transformation with 3-s time resolution at the central frequency 1 Hz (as calculated by the full width at half maximum; FWHM) was used to calculate spectral power estimates at each point of the time-frequency window ranging from -2s to 2s (20 ms steps) in the time domain and 1 to 40 Hz (1 Hz steps) in the frequency domain. TFRs were baseline corrected with respect to the power averaged over the entire epoch.

EEG analyses

Neural encoding of emotion and color intensity

To test Hypothesis 1 of an earlier selective neural encoding of threat-related information during the emotion vs. the color task, generalized linear regression models (GLM) were used, where emotion or color strength (from 0 for a neutral expression/gray to 7 for an intense anger expression/violet) was introduced as a trial-per-trial predictor of broadband EEG signals at each electrode and time point following stimulus presentation.[36,107] We added the choice as an additional regressor to control for participants' subsequent detection reports (detection of violet in the color task, detection of anger in the emotion task) on a trial-by-trial basis. The corresponding parameter estimates of the regression, reported in arbitrary units, were calculated per participant, and then averaged across participants to produced group-level averages. The resulting time course at each electrode of the parameter estimates represents the degree to which the EEG activity 'encodes' (co-varies

with) the emotion or color strength provided by the morphed facial features or color intensity. The strength of this neural encoding– indexed by the amplitude of the parameter estimate– provides a measure of the neural sensitivity to emotion or color strength.

We conducted this analysis separately for the emotion task (regressor: emotion intensity) and the color task (regressor: color intensity) and performed a multiple comparison correction on one-sample t-tests comparing parameter estimates against zero (null effect), to isolate the electrodes and timepoints where neural encoding of intensity was significant (Table 1). To do so, we used Fieldtrip's multiple comparison analysis,[108] using the MonteCarlo method to calculate the probability of significance, dependent sample T-statistics, cluster corrections (clusteralpha = 0.005, cluster statistic = maxsum, correct tail = prob, number of permutations = 1500). We also conducted this multiple comparison analysis on the difference between the parameter estimates for emotion encoding and color encoding (see Table 1). Finally, to test our Hypothesis 3a, we did the same analysis for emotion encoding in the emotion task, this time isolating facial expressions with a direct gaze and those with an averted gaze (see Table 2). As in the emotion vs. color tasks, here we corrected for multiple comparisons for the effects against zero, and for the differences between the two conditions (gaze direct vs. gaze averted).

Prediction of choice with motor lateralization

To test hypothesis 2, we assessed whether and when the detection of choice can be predicted by the motor lateralization activity in the mu-alpha (8–12 Hz) and -beta (12–32 Hz) frequency bands (30). To compute the motor lateralization activity, we first isolated effector-selective (left vs. right hand) neural activity. As mu-beta activity is known to be suppressed at response time in the hemisphere contralateral to the hand used for response,[31,62] we calculated the spectral power from 8 to 12 Hz or 12 to 32 Hz at response time for each electrode and time point for all subjects, for both emotion and color decisions. The resulting response-locked mu-alpha or beta activity for the trials in which subjects responded with their right hand was then subtracted from that of trials in which subjects responded with their left hand. After averaging across all subjects, the electrodes where the motor lateralization was maximal at 200 ms before response time were identified at 'P3','CP3','C3' for the left hemisphere and 'P4','CP4','C4' for the right hemisphere for both types of decisions. For emotion/color decisions, motor lateralization activity specific to 'anger'/'violet' responses was obtained by subtracting contralateral from ipsilateral mu spectral activity (8-12 Hz or 12-32 Hz) relative to the hand assigned to 'anger'/'violet' responses (counterbalanced across subjects), over effector-selective electrodes at each time point for all subjects. We then performed a logistic regression to predict choice (Anger/Neutral in the emotion task, Violet/Gray in the color task) with the trial-by-trial motor lateralization activity as predictor, and trial-by-trial reaction times as an additional regressor to isolate for effects that are independent of participants' fluctuations in response times and differences in RTs between the two tasks.

$$\log\left(\frac{choice(anger\ or\ neutral)}{1 - choice_{(anger\ or\ neutral)}}\right) = \beta_0 + \beta_1 \cdot EEG_{lat\ idx} + \beta_2 \cdot RT$$

$$\log\left(\frac{choice(violet\ or\ gray)}{1 - choice_{(violet\ or\ gray)}}\right) = \beta_0 + \beta_1 \cdot EEG_{lat\ idx} + \beta_2 \cdot RT$$

We extracted and plotted the parameter estimates of this regression over time (see Figure 3C) and compared the parameter estimates predicting the response Anger with the parameter estimate predicting the response Violet at each time point using a paired samples t-test. We corrected for multiple comparisons by randomly shuffling the pairings between responses and EEG signals 1000 times. The maximal cluster-level statistics (the sum of t-values across contiguous significant time points at a threshold level of 0.05) were extracted for each shuffle to compute a 'null' distribution of effect size across the [-200, +1100]ms time window. For the significant cluster in the original data, we computed the proportion of clusters in the null distribution whose statistic exceeded that obtained for the cluster in question, corresponding to its 'cluster-corrected' p.

To test our hypothesis 3b, we predicted the response 'anger' with the motor preparation measure in the mu-alpha band on the mean activity of the isolated significant cluster from 240 ms to 380 ms, separately for direct and averted gaze.